NIH Public Access
Author Manuscript
J Nat Prod. Author manuscript; available in PMC 2009 September 1.

Published in final edited form as:
J Nat Prod. 2008 September ; 71(9): 1544–1550. doi:10.1021/np800110e.

Viridamides A and B, Lipodepsipeptides with Anti-Protozoal Activity from the Marine Cyanobacterium *Oscillatoria nigro-viridis*

Thomas L. Simmons[†], **Niclas Engene**[†], **Luis David Ureña**[‡], **Luz I. Romero**[‡], **Eduardo Ortega-Barría**[‡], **Lena Gerwick**[†], and **William H. Gerwick**[†,*]

†*Scripps Institution of Oceanography and Skaggs School of Pharmacy and Pharmaceutical Sciences, University of California San Diego, La Jolla, CA 92093-0212*

‡*Institute for Advanced Scientific Investigation and High Technology Services, Secretariat of Science and Technology, Clayton, Ancon, Republic of Panama*

Abstract

Parallel chemical and phylogenetic investigation of a marine cyanobacterium from Panama led to the isolation of two new PKS-NRPS derived compounds, viridamides A and B. Their structures were determined by NMR and mass spectroscopic methods, and the absolute configurations assigned by Marfey's method and chiral HPLC analysis. In addition to six standard, *N*-methylated amino and hydroxy acids, these metabolites contained the structurally novel 5-methoxydec-9-ynoic acid moiety and an unusual proline methyl ester terminus. Morphologically, this cyanobacterium was identified as *Oscillatoria nigro-viridis*, and its 16S rDNA sequence is reported here for the first time. Phylogenetic analysis of these sequence data has identified *O. nigro-viridis* strain OSC3L to be closely related to two other marine cyanobacterial genera, *Trichodesmium* and *Blennothrix*. Viridamide A showed anti-trypanosomal activity with an IC_{50}= 1.1 μM and anti-leishmanial activity with an IC_{50} = 1.5 μM.

The World Heath Organization (WHO) estimates that over 1 billion people suffer from one or more neglected tropical diseases (NTDs) such as malaria, leishmaniasis, trypanosomiasis, schistosomiasis, cholera and others.[1] On a global scale NTDs account for greater than 10% of global disease burden yet only 16 of the 1393 new drugs marketed between 1975 and 1999 were developed for their treatment.[2] A major cause for this extraordinarily unimpressive number is the fact that those people most burdened by these diseases are amongst the World's most impoverished.[3]

Trypanosomiasis (Chagas' disease, sleeping sickness) and leishmaniasis are caused by infection by parasitic members of the protozoan order *Trypanosomatida* which enter the blood stream via insect vectors or transfusion of infected blood.[4] Symptoms of Chagas' disease occur in two phases: an acute stage characterized by localized swelling and fever, and a chronic stage which may develop over a decade or more. Chronic stage infection, if left untreated, results in protozoan infestation of all major organs leading to neurological disorders, intestinal damage and fatal cardiomyopathy. Leishmaniasis is caused by 20 different species and can affect humans as three forms: visceral (VL; 'kala azar'), cutaneous and mucocutaneous. The pan-tropical phlebotomine sand fly is the known vector of leishmaniasis, with VL being the most severe disease form. If untreated visceral leishmaniasis can be 100 % lethal within two years.[5] The WHO estimates that more than 200 million people are at risk of leishmaniasis or trypanosomiasis worldwide.[6,7] Several drugs are currently available and used to treat

*To whom correspondence should be addressed. Tel.: (858) 534-0578. Fax: (858) 534-0529. E-mail: wgerwick@ucsd.edu.

NIH-PA Author Manuscript
NIH-PA Author Manuscript
NIH-PA Author Manuscript

NIH-PA Author Manuscript

NIH-PA Author Manuscript

NIH-PA Author Manuscript

trypanosomal infections; however, all of these suffer from one or more shortcomings,[8,9] and drug resistance is emerging and threatens their utility.[10] Despite the pressing and obvious global need for new and more effective anti-protozoal medicines, no new drugs are currently being developed for the treatment of these pan-tropical diseases.[11] In addition, while drug discovery programs are making some advances against these pathogens, for example with synthetic phospholipids, progress is slow and the treatments are expensive with many undesirable side effects.[12]

As part of a Panama-based International Cooperative Biodiversity Group (ICBG) project, we have been evaluating the extracts of tropical marine plants, endophytic fungi, and marine algae and cyanobacteria for activity against several tropical parasitic diseases including malaria, leishmaniasis, and Chagas' disease.[13] Marine cyanobacteria are extremely rich in diverse lipopeptide natural products, many of which have potent biological activities.[14] In the process of adapting a collection of the marine cyanobacterium *Lyngbya majuscula* to laboratory culture, collected from near the island of Curaçao, a second contaminating cyanobacterium was also isolated. This was cultured in scaled-up quantities and its extract examined for unusual secondary metabolites by LCMS and NMR screening. Subsequently, these efforts were rewarded by the discovery of two novel lipopeptides, termed viridamide A (**1**) and B (**2**). Evaluation of these in our suite of tropical disease assays in Panama identified the major component, viridamide A, to be nearly equipotent at inhibiting the parasites causing leishmania and Chagas' disease (IC_{50} = 1.1 and 1.5 μM, respectively).

An additional dimension of this study involved a detailed investigation into the taxonomic identity of the viridamide-producing strain of cyanobacterium. Based on its gross morphology we reasoned that this strain was dissimilar to those we had previously worked with and that this presented an opportunity to broaden our base of natural product-rich cyanobacteria genera for future studies. Hence, we engaged in a two-pronged investigation using both traditional morphological characters and 16S rDNA sequence information. However, in the course of these studies, we realized a number of problems in the phylogenetic approach, mainly due to a) the level of sequence conservation of the 16S rRNA gene is too high for precise species differentiation, and b) the general unavailability of 16S rDNA sequence data for many of the morphologically-defined species of cyanobacteria. In response to the first point above, we used the present study as an opportunity to explore additional genes in cyanobacteria that could improve the phylogenetic analysis. In response to the second issue, we and others are actively engaged in expanding the availability of 16S rRNA gene sequences which are well correlated to morphologically described species.[15] This two-pronged approach has allowed us to identify the source of the viridamides as the marine cyanobacterium *Oscillatoria nigro-viridis*, and to describe its phylogenetic relationship to other genera and species of marine cyanobacteria.

Results and Discussion

Isolation and structure elucidation of the viridamides

The dark green and very small cyanobacterial filaments of strain OSC3L (10 μm wide by > 1 cm long) were isolated as a contaminating (epiphytic) species from a partially purified culture of *Lyngbya majuscula* 3L (GenBank acc. No. AY599501) collected at the CARMABI Research Station in Curacao, Netherlands Antilles in 1993. The filaments of OSC3L were isolated on solid agar plates using standard isolation techniques and then cultured in enriched seawater medium under cool white fluorescent lights for 21 days. Harvest of filaments was achieved by filtration through paper filters, and extraction and initial fractionation was performed using our standard protocols.[16] Screening of fractions by LCMS and NMR showed two mid-polar fractions to contain interesting metabolites, and two compounds, named viridamide A (**1**) and B (**2**), were subsequently isolated by repetitive reversed-phased HPLC in 1.9% (30 mg) and 0.2% (3.6 mg) yield, respectively.[17]

NIH-PA Author Manuscript

NIH-PA Author Manuscript

NIH-PA Author Manuscript

Viridamide A (**1**) was isolated as a colorless glassy oil with a molecular formula of $C_{46}H_{79}N_5O_{10}$ as determined by HR ESI TOF MS (obsd $[M+H]^+$ at *m/z* 862.5847; calcd $[M+H]^+$ 862.5827). This formula agreed with deductions from the ^1H and ^{13}C NMR data (Table 1), and corresponded to 10 degrees of unsaturation. FT-IR absorption peaks at 1640 and 1750 cm^{-1} indicated the presence of amide and ester functionalities, respectively. The ^1H NMR spectrum of **1** was well dispersed in $CDCl_3$ and displayed a pattern of chemical shifts typical for peptides (two NH doublets at δ_H 6.21 and 6.45 and a series of α-amino and α-hydroxy protons at δ_H 4.37–5.0). Two 3H singlets at δ_H 3.01 and 3.07 indicated the presence of two *N*-methylated amides whereas two sharp methyl singlets at δ_H 3.29 and 3.64 were consistent with two methoxy groups. The ^{13}C NMR spectrum of **1** displayed all 46 carbon resonances, and seven of the 10 double bond equivalents were attributable to seven ester/amide carbonyl resonances between 160 and 175 ppm. Carbon resonances at δ_C 68.4 and 84.3, in combination with gHMBC data, were determined to comprise a terminal acetylenic group, and thus accounted for an additional two degrees of unsaturation. These data suggested viridamide A contained a single ring.

Interpretation of two dimensional NMR spectra (gCOSY, gHSQC, and gHMBC) defined partial structures for an *N*-methylisoleucine, two valine residues, an *N*-methylvaline, a 2-hydroxy-3-methylpentanoic acid residue, and a terminal proline methylester (Table 1). These structural fragments accounted for 680 Da, leaving $C_{11}H_{17}O_2$ still to be determined. Further analysis of the 2D-gHSQC-TOCSY NMR data revealed seven continuously coupled protons beginning with one at δ_H 2.20 (δ_C 36.6) and correlated to δ_H 1.67 (δ_C 21.5), δ_H 1.48 (δ_C 32.8), δ_H 3.15 (δ_C 80.1), δ_H 1.56 (δ_C 32.3), δ_H 1.55 (δ_C 24.1), and δ_H 2.18 (δ_C 18.5). Combining these TOCSY data with gCOSY and gHMBC interpretations allowed development of a structurally-novel methoxylated fatty acid moiety, 5-methoxydec-9-ynoic acid (Mdyna, Figure 1). These seven partial structures accounted for all atoms present in the molecular formula of viridamide A (**1**)(see Table 1).

The linear sequence of the assigned partial structures was determined by combined 1D-HMBC and FAB-MS/MS fragmentation patterns. Interpretation of the HMBC correlations from the α-amino and α-hydroxy proton resonances (4–5 ppm) to the adjacent carbonyl carbons, and from the two amide protons to their adjacent carbonyl carbons, allowed the assembly of a linear sequence for most of viridamide A (**1**). A 1D HMBC experiment was used to observe correlation from H-5 through the oxygen atom to the adjacent C-12 ester carbonyl resonance. Interpretation of the FAB MS/MS fragmentation pattern fully supported the linear sequence proposed from the HMBC analysis.

The absolute configurations of the α-amino and α-hydroxy acid residues in viridamide A were determined by combined chiral HPLC [for Val, *N*-Me-Val, Pro, and 2-hydroxyl-3-methylpentanoic acid (HMPA)] and application of the advanced Marfey's method (*N*-Me-Ile).[18,19] Chiral HPLC was achieved using a dioctyl-(D)-penicillamine (Chirex 3126; Phenomenex) column with aqueous 2.0 mM $CuSO_4$ in CH_3CN. Comparison of retention times for the acid hydrolysate of **1** (6 N HCl at 110° for 18 hours) with authentic standards indicated an L-configuration for the Val, *N*-Me-Val, Pro and HMPA residues. Configurational assignment of the *N*-Me-Ile required division of a portion of the acid hydrolysate and derivatization of each with either L- or D-FDAA (1-fluoro-2,4-dinitrophenyl-5-alanine amide) to produce the chromatographic equivalents of D-*N*-Me-Ile and L-*N*-Me-Ile. Reverse-phase HPLC of the FDAA derivatives indicated an L-(2*S*, 3*S*)-configuration for this residue.

Viridamide B (**2**) was isolated as a colorless oil with a molecular formula of $C_{45}H_{77}N_5O_{10}$ as determined by HR-TOF-MS (obsd $[M+H]^+$ at *m/z* 848.5661; calcd $[M+H]^+$ 848.5670), and this molecular formula was also supported by the ^1H and ^{13}C NMR data (Table 2). The ^1H and ^{13}C NMR spectra of **2** closely resembled those of viridamide A (**1**); however, there was a

NIH-PA Author Manuscript

NIH-PA Author Manuscript

NIH-PA Author Manuscript

notable absence of a high field methyl carbon resonance in the 10–11 ppm range, assigned to the C-10 methyl of the HMPA residue in **1**, and this appeared to explain the 14 Da mass reduction found between the two compounds. Analysis of the 2D gHSQC and gHMBC NMR spectra of **2** revealed that viridamide B contained a 2-hydroxy-3-methylbutanoic acid (HMBA) residue versus the 2-hydroxy-3-methylpentanoic acid residue found in viridamide A. The remaining structural features were identical between the two metabolites as determined by detailed NMR and MS analysis. Because viridamide B was isolated in much smaller yield that viridamide A, its absolute configuration was not studied experimentally; however, based on its co-occurrence with A and nearly identical structural and NMR features, we predict it possesses the same configuration at comparable centers.

Biological Evaluation of viridamide A

Inspired by the bioactivity of other recently discovered linear peptides of cyanobacterial origin,[13, 20] viridamide A (1) was tested against a series of relevant tropical pathogens and cancer cell lines. Interestingly, **1** displayed significant activity against the three parasitic protozoa *Trypanosoma cruzi*, *Leishmania mexicana* and *Plasmodium falciparum* with little toxicity to the cancer cell lines treated. The assay results are summarized in Table 3. The variable toxicity between pathogen and human derived cell lines is encouraging and may suggest therapeutic value for these new compounds. Studies are ongoing to more fully understand these results.

Mophological and phylogenetic characterization of the viridamide-producing cyanobacterium

The culture sample of strain OSC3L was observed as a blackish-green, mat-forming, filamentous cyanobacterium. Microscopically, it possessed cylindrical trichomes that were straight or slightly waved that measured 9–10 μm wide. The trichomes were covered with a thin, barely visible sheath and there were slight constrictions at the cross walls between cells. The cells were disk-shaped with a cell length (2–3 μm) to width (9–10 μm) ratio of approximately 0.25, and were granulated near the crosswalls. The terminal cells were capitated and the trichomes slightly attenuated towards their tips. On the basis of these morphological features, strain OSC3L was identified as *Oscillatoria nigro-viridis* Thwaites in Harvey.[21]

To gain further insight into the phylogenetic relationship of this collection of *O. nigro-viridis* to other species and genera of cyanobacteria, a detailed molecular genetic analysis was conducted of strain OSC3L by amplifying its nearly full length 16S rRNA gene sequence using cyanobacterial specific primers (1378 bp, 93% of 16S gene; GC content 54.79%; GenBank acc. No. EU244875). Because characterization of the species *O. nigro-viridis* is based entirely on a morphological description, a 16S rRNA gene sequence was not available for comparison with our data (e.g. this is the first report of the 16S rRNA gene sequence for this species). However, BLAST analysis revealed this gene sequence to be 99.3% identical to that of a filamentous cyanobacterium (strain PAB-21) we recently collected from the Caribbean coast of Panama (GenBank acc. No. EU253967). This latter collection was also characterized as an *Oscillatoria* sp. based on its morphological features. In addition, BLAST analysis showed that strain OSC3L was phylogenetically closely related to several other *Oscillatoria* and *Trichodesmium* strains, including *T. erythraeum* IMS101 (97.4%; GenBank acc. No. CP000393) and *O. sancta* PCC 7515 (97.2%; GenBank acc. No. AF132933).

Phylogenetic trees were constructed from the 16S rDNA gene sequence obtained for strain OSC3L and related sequences recovered from Genbank following the BLAST analysis. Three commonly employed algorithms for constructing phylogenetic trees were used in this analysis (parsimony, distance, and maximum likelihood; see Methods and Supporting Information), and all gave very similar topologies. However, the maximum-likelihood method (ML)

NIH-PA Author Manuscript

NIH-PA Author Manuscript

NIH-PA Author Manuscript

provided the most robust boot-strap values and thus was used to construct the phylogenetic tree shown in Figure 4.

As predicted from the BLAST analysis, strain OSC3L clusters in a distinct and well boot-strap supported monophyletic clade that contains various strains of *Oscillatoria* and *Trichodesmium*.

O. nigro-viridis OSC3L groups closely with other strains of *Trichodesmium* and *Oscillatoria*. This clade is described in Bergey's manual as the *Trichodesmium-Oscillatoria* lineage.[22,13] Recently, it was shown that the genus *Blennothrix* (former *Hydrocoleum* sensu *Komárek & Anagnostidis, 2005*; *B. cantharidosmum* GenBank acc. No. EU253967) also clades within the *Trichodesmium-Oscillatoria* lineage and this has led to a proposal that these genera derive from a common evolutionary origin.[23] While several strains of *Oscillatoria*, *Trichodesmium*, and recently *Blennothrix*, have been associated with the production of biological active secondary metabolites,[15,24] the genus *Oscillatoria* is clearly the richest in this regard.[25] *O. nigro-viridis* contributes to Harmful Alga Blooms (HABs) by causing dermatitis and inflammation in humans,[26] and is reported to have fish anti-feedant properties.[27] Chemical analyses of Pacific strains of *O. nigro-viridis* have yielded several bioactive compounds, including debromoaplypsiatoxin, oscillatoxin A, 21-bromooscillatoxin A, 19,21-dibromooscillatoxin A, and 19-bromoaplysiatoxin, a suite of metabolites which likely explains the toxic effects of this species in humans.[28] Whether these reports truly reflect a greater ability of *Oscillatoria* to produce natural products versus *Trichodesmium* and *Blennothrix*, or rather, identifies that benthic cyanobacteria have been better studied than those with a mainly planktonic habit, is uncertain at present. Ongoing studies which partner detailed culture, chemical, pharmacologic and phylogenetic investigations should give valuable insights into this important question.

Conclusions

Herein we report two new bioactive marine natural products, viridamides A (**1**) and B (**2**), as well as details of the molecular taxonomy of the producing marine cyanobacterium. These new viridamide natural products have a familiar overall topology compared with other cyanobacterial metabolites, such as the carmabins,[29] jamaicamides,[30] and apramides,[31] in that they are linear lipopeptides with a terminal acetylene group. However, they also display unique structural modifications within this sub-group in that they contain a terminal proline methyl ester and 5-methoxydec-9-ynoic acid moiety. Viridamide A show anti-trypanosomal activity (IC_{50}= 1.1 μM to *Trypanosoma cruzi*) and anti-leishmanial activity (IC_{50} = 1.5 μM to *Leishmania mexicana*), and thus represents a moderately potent new chemotype to display activity to these important parasitic diseases. Our combined morphological and molecular phylogenetic approaches to characterize the producing strain of cyanobacterium, *O. nigro-viridis*, as well as reveal its taxonomic relationships to other cyanobacterial species, allows for a deeper understanding and appreciation of the biological and chemical diversity in this taxonomic group. In turn, these insights are being employed to refine and make more productive our continuing drug discovery efforts.

Experimental Section

General Experimental Procedures

Optical rotations were measured using a Perkin-Elmer 241 polarimeter with a 10 cm cell. UV spectra were recorded on a Waters model 996 LC photodiode array detector and IR spectra on a ThermoElectron Nicolet IR100 FT-IP spectrometer. ^{1}H and 2D NMR data were obtained on a Varian Inova spectrometer operating at 500 MHz. ^{13}C NMR spectra were acquired on a Varian Inova spectrometer operating at 75 MHz. $CDCl_3$ residual solvent peaks were used as

NIH-PA Author Manuscript

NIH-PA Author Manuscript

NIH-PA Author Manuscript

internal references (δ_H 7.26; δ_C 77.0 ppm). Low resolution LC/MS and MS/MS data were acquired on a Thermo Finnigan LCQ Advantage Max spectrometer with ESI source and Surveyor Series LC. The FAB mass spectrum was recorded on Kratos MS50TC mass spectrometer. High resolution mass spectra were collected on a high accuracy Agilent ESI-TOF at the Scripps Research Institute, La Jolla, CA.

Collection, Isolation and Culture of *Oscillatoria nigro-viridis* strain OSC3L

Strain OSC3L was isolated from an assemblage of *Lyngbya majuscula* collected at the CARMABI Research Station in Curaçao, Netherlands Antilles in 1993. The OSC3L filaments were isolated on solid agar plates using standard isolation techniques, as previously described.[32] The isolated OSC3L filaments were cultured in BG-11 medium at 28°C with 33 g/L Instant Ocean salt (Aquarium Systems, Mentor). The cultures were kept in a 16 h/8 h light/dark cycle with a light intensity of *ca.* 500 LUX provided by 40W cool white fluorescent lights. Scaled-up cultures for organic extraction or DNA extraction were produced using 75 ml Erlenmeyer flasks, 3 L Fernbach flasks and 15 L pans, with the medium changed every 21 days. Total culture time varied from 21 to 30 days.

Isolation of Viridamides A (1) and B (2)

The crude extract (1.56 g) was fractionated by normal phase vacuum liquid chromatography (VLC) on Si gel resulting in nine fractions of increasing polarity (A, 100% hexanes; B, 10% EtOAc in hexanes; C, 20% EtOAc in hexanes; D, 40% EtOAc in hexanes; E, 60% EtOAc in hexanes; F, 80% EtOAc in hexanes; G, 100% EtOAc; H, 25% CH_3OH in EtOAc; I, 100% CH_3OH). These nine fractions and the crude extract were then simultaneously screened by NMR and LC MS and evaluated for cancer cell cytotoxicity. The parallel screening of fractions G and H indicated the presence of unknown compounds and showed cytotoxicity in the initial screen.[10] These fractions were subjected to RP C_{18} HPLC (Phenomenex RP-Fusion semi preparative column 10 × 250 mm) monitored at 254 nm; 45 min gradient elution 80% aq CH_3OH to 100% CH_3OH at 3.0 mL/min flow rate). Viridamides A and B (30 and 3.6 mg, respectively) were further purified from the fractions eluting at 19.5 and 17.5 min, respectively, by repeated isocratic HPLC (Phenomenex RP-Fusion semi preparative column 10 × 250 mm; CH_3CN: H_2O (7:3) at 3.0 mL/min.

Viridamide A (1)—colorless oil; $[\alpha]_D$ -107.4 (*c* 0.05, $CDCl_3$); UV (CH_3CN) λ_{max} (log ε) 210 (2.9); IR (neat) ν_{max} 3500, 3313, 2962, 2971, 2873, 1737, 1643, 1533, 1461, 1442, 1192, 1100, 1011 cm^{-1}; ^1H NMR (500 MHz, $CDCl_3$) and ^{13}C NMR (75 MHz, $CDCl_3$), see table 1; FAB MS *m/z* 735.51 ($C_{40}H_{69}N_4O_8$), 608.45 ($C_{35}H_{62}N_5O_8$), 454.29 ($C_{23}H_{40}N_3O_6$), 407.29 ($C_{23}H_{39}N_2O_4$), 355.22 ($C_{18}H_{31}N_2O_5$), 280.22 ($C_{17}H_{30}NO_2$); HR ESI TOF MS (obsd $[M+H]^+$ at *m/z* 862.5847; calcd $[M+H]^+$ 862.5827).

Viridamide B (2)—colorless oil; $[\alpha]_D$ -98 (*c* 0.10, $CDCl_3$); UV (CH_3CN) λ_{max} (log ε) 210 (3.1); IR (neat) ν_{max} 3500, 3313, 2962, 2971, 2873, 1737, 1643, 1533, 1461, 1442, 1192, 1100, 1011 cm^{-1}; ^1H NMR (500 MHz, $CDCl_3$) and ^{13}C NMR (75 MHz, $CDCl_3$), see table 2; HR TOF MS (obsd $[M+H]^+$ at *m/z* 848.5661; calcd $[M+H]^+$ 848.5670)

Acid Hydrolysis, Chiral HPLC, and Advanced Marfey's Analysis

Viridamide A (1 mg) was hydrolyzed in 0.5 mL of 6N HCl at 110°C for 18 h. Excess aq HCl was removed under vacuum. The dry material was resuspended in 0.5 mL of H_2O. Retention time comparisons of the commercially available L- and D- free amino acids by chiral HPLC (Chirex 3126, UV detection at 245 nm), indicated an L-configuration for all residues. L-Ile with 85:15 2 mM $CuSO_4$/CH_3OH) (15.4 min; L-*allo*-Ile, 12.9 min; D-Ile, 24.3 min; D-*allo*-Ile 20.0 min), L-Val with 2 mM $CuSO_4$ (23.0 min; D-Val, 36.1 min), *N*-Me- L-Val with 2 mM

NIH-PA Author Manuscript

NIH-PA Author Manuscript

NIH-PA Author Manuscript

$CuSO_4$ (15.5 min; *N*-Me- D-Val, 24.8 min), L-Pro with 2 mM $CuSO_4$ (18.2 min; D-Pro, 32.3 min).

For determination of the configuration of the *N*-Me-Ile residue, the hydrolysate of **1** was divided into two portions and dissolved in 1N $NaHCO_3$ (100 μL) followed by the separate addition of 50 μL of 3 mg/mL (acetone) L-FDAA and D-FDAA, respectively. The reaction mixture was incubated at 80°C for 3 min, then quenched by neutralization with 50 μL of 2N HCl. Next, 300 μL of 50% aq CH_3CN was added to the solution and the products were analyzed by reversed-phase HPLC (LiChrosphere 100 C_{18}, UV detection at 340 nm) using a linear gradient of 9:1 50 mM triethylammonium phosphate (TEAP) buffer (pH 3)/CH_3CN to 1:1 TEAP/CH_3CN over 60 min. Because only *N*-Me-L-Ile and *N*-Me-L-*allo*-Ile were commercially available, the D-Marfey's reagent was used to make the *N*-Me-D-Ile and *N*-Me-D-*allo*-Ile chromatographic equivalents. The retention times (t_R, min.) of the Ile derivative from the hydrolysate of **1** matched that of *N*-Me-L-Ile, (40.7 min ; *N*-Me-L-*allo*-Ile, 41.2 min; *N*-Me-D-Ile, 44.2 min; *N*-Me-D-*allo*-Ile, 44.7 min).

Preparation and chiral analysis of HMPA

L-Ile (100 mg, 0.75 mmol) was dissolved in 50 mL 0.2 N $HClO_4$ at 0°C. To this was added a cold (0°C) solution of $NaNO_3$ (1.4 g, 20 mmol) in 20 mL H_2O with rapid stirring. With continued stirring the reaction mixture was allowed to reach room temperature at which time evolution of N_2 subsided (*ca.* 30 min). The solution was then boiled for 3 min, cooled to room temperature, and then saturated with NaCl. This mixture was extracted with Et_2O and dried under vacuum. The three other stereoisomers (2*R*, 3*R*)-HMPA, (2*R*, 3*S*)-HMPA, and (2*S*, 3*R*)-HMPA were synthesized in a similar manner from D-Ile, D-*allo*-Ile, and L-*allo*-Ile, respectively. A portion of the resultant oil was dissolved in aq 2 mM $CuSO_4$ buffer for HPLC. The retention time (Chirex-D, linear gradient 100:0 2 mM $CuSO_4$: CH_3CN to 95:5 over 20 min) of the natural product hydrolysate matched that for 2*S*,3*S*-HMPA (18.7 min; 2*R*,3*S*-HMPA, 15.2 min; 2*S*,3*R*-HMPA and 2*R*,3*R*-HMPA, 23.2 min).

Intracellular *T. cruzi* Assay

The anti-trypanosomal activity was determined using a recombinant Tulahuen clone C4 of *Trypanosoma cruzi* that expresses β-galactosidase as a reporter enzyme.[33] The method is based on the growth inhibition effect of test samples on trypomastigote, the intracellular form of the parasite, infecting Vero cells, as previously described.[34]

Anti-leishmanial Bioassay

Leishmaniasis bioassays were performed using a method based on parasite (*Leishmania mexicana*) DNA fluorescence, as previously described.[35]

Morphological Analysis of strain OSC3L

The morphological characterization of OSC3L was performed using an Olympus BH-2 light microscope. The following parameters were selected to describe its morphology: length, width and length/width ratios of vegetative cells, presence/absence of specialized cells such as heterocysts, akinetes or calyptra, the size and shape of trichomes, granulation, constrictions at cross-walls, morphology of terminal cells, and thallus growth characteristics and coloration. Morphological identification was made in accordance with traditional phycological[20] and bacteriological systems.[18]

DNA extraction, 16S rRNA gene PCR-amplification and Cloning

Genomic DNA was extracted from 40 mg of cleaned algal tissue using the Wizard® Genomic DNA Purification Kit (Cat. A1120) following the manufacturer's specifications (Promega,

NIH-PA Author Manuscript

NIH-PA Author Manuscript

NIH-PA Author Manuscript

Madison, WI). The isolated genomic DNA was further purified using a Genomic-tip 20/G kit from Qiagen® (Cat. 10223). The 16S rRNA gene was amplified from isolated DNA using the cyanobacterial-specific primers, 106F and 1509R, as previously described.[21] The reaction volume was 25 μL containing 0.5 μL of DNA (50 ng), 2.5 μL of 10 × PfuUltra IV reaction buffer, 0.5 μL of dNTP mix (25 mM each of dATP, dTTP, dGTP, and dCTP), 0.5 μL of each primer (10 μM), 0.5 μL of PfuUltra IV fusion HS DNA polymerase (Cat. 600760) and 20.25 μL dH2O. The PCR reaction was performed in an Eppendorf® Mastercycler® gradient as follows: initial denaturation for 2 min at 95°C, 30 cycles of amplification: 20 sec at 95°C, 20 sec at 50°C and 1.5 min at 72°C, and final elongation for 3 min at 72°C. PCR products were subcloned using the Zero Blunt® TOPO® PCR Cloning Kit (Cat. K2800-20SC) from Invitrogen, into the pCR®-Blunt IV TOPO® vector, and then transformed into TOPO® cells and cultured on LB-kanamycin plates. Plasmid DNA was isolated using the QIAprep® Spin Miniprep Kit (Cat. 27106) from Qiagen and sequenced with pCR®-Blunt IV TOPO® vector specific primers M13F/M13R and internal middle primers 359F and 781R as previously described.[21]

Phylogenetic Analysis of Strain OSC3L

The bi-directional 16S rRNA gene sequences of OSC3L were combined and the resulting consensus sequence was inspected both visually and by secondary structure analysis using the CLC DNA Workbench 3. The GC content was determined using the MBCF Oligo Calculator from the Dana-Farber Cancer Institute, Molecular Biology Core Facilities (http://mbcf.dfci.harvard.edu/docs/oligocalc.html). The 16S rRNA gene was aligned together with related cyanobacterial strains representing 13 major genera of the order *Oscillatoriales* (subsection III) obtained from GenBank (http://www.ncbi.nlm.nih.gov) and the Ribosomal Database Project II (http://rdp8.cme.msu.edu/html/). The multiple sequence alignments were performed using ClustalX in MEGA 4[36] with standard gap opening and extension penalties without gaps. The aligned 16S rRNA gene sequences were used to generate phylogenetic trees in MEGA 4. The phylogenetic relation of the cyanobacterial 16S rDNA genes were compared by (1) the distance method by Neighbor-Joining (NJ), (2) Maximum Parsimony (MP), and (3) the Maximum-Likelihood (ML) method. The evolutionarily distant cyanobacterium *Nostoc punctiforme* PCC73102 (GenBank acc. No. AF027655), from the order Nostocales, was used as an outgroup. Selection of the phylogenetic method used for the tree appearing in Figure 4 was based on tree topology and boot-strap values.

Supplementary Material

Refer to Web version on PubMed Central for supplementary material.

Acknowledgment

We gratefully acknowledge the government of Curaçao for permission and the Carmabi Research Station for assistance in making these cyanobacterial collections. We thank R.C. Coates for cyanobacterial culturing, and M. Balunas and C. Spatafora for assistance with data management. Financial support for this work came from the National Cancer Institute (CA52955) and the International Cooperative Biodiversity Groups Program (grant number 1U01 TW 006634-01).

References

1. http://www.who.int/neglected_diseases/en/
2. Trouiller P, Olliara P, Torreele E, Orbinski J, Laing R, Ford N. Lancet 2002;359:2188–2194. [PubMed: 12090998]
3. Yamey G. Br. J. Med 2002;325:176–177.
4. Teixeira ARL, Nascimento RJ, Sturm NR. Mem. Inst. Oswald Cruz, Rio de Janeiro 2006;101:463–491.

NIH-PA Author Manuscript

NIH-PA Author Manuscript

NIH-PA Author Manuscript

5. www.who.int/leishmaniasis/en/
6. Guerin PJ, Olliaro P, Sundar S, Boelaert M, Croft SL, Desjeux P, Wasunna MK, Bryceson ADM. Lancet Infect. Dis 2002;2:494–501. [PubMed: 12150849]
7. World Health Organization. Technical Report Series. Geneva: WHO; 2002. Control of Chagas disease: second report of the WHO expert committee.
8. Sanderson L, Khan A, Thomas S. Antimicrob. Agents Chemother 2007;51:3136–3146. [PubMed: 17576845]
9. (a) Lee J, Michael AJ, Martynowski D, Goldsmith EJ, Phillips MA. J. Biol. Chem 2007;282:27115–27125. [PubMed: 17626020] (b) Priotto G, Kasparian S, Nqouama D, Ghorashian S, Arnold U, Ghabri S, Karunakara U. Clin. Infect. Dis 2007;45:1435–1442. [PubMed: 17990225]
10. Carrillo C, González NS, Algranati ID. Biochimica et Biophysica Acta 2007;1770:1605–1611. [PubMed: 17920200]
11. Bouteille B, Oukem O, Bisser S, Dumas M. Fundam. Clin. Pharmocol 2003;17:171–181.
12. Seifert K, Lemke A, Croft SL, Kayser O. Antimicrob. Agents Chemother 2007;51:4525–4528. [PubMed: 17908944]
13. (a) Sanchez LA, Capitan Z, Romero LI, Ortega-Barria E, Gerwick WH, Cubilla-Rios L. Nat. Prod. Commun 2007;2:1065–1069. (b) McPhail KL, Correa J, Linington RG, Gonzalez J, Ortega-Barria E, Capson TL, Gerwick WH. J. Nat. Prod 2007;70:984–988. [PubMed: 17441769]
14. Gerwick, WH.; Tan, L.; Sitachitta, N. The Alkaloids. Vol. Vol. 57. San Diego: Academic Press; 2001. p. 75-184.
15. (a) Marquardt J, Palinska KA. Archives of Microbiol 2007;5:397–413.187 (b) Rajaniemi P, Hrouzek P, Kaštovská K, Willame R, Rantala A, Hoffmann L, Komárek J, Sivonen K. Int. J. Syst. Evol. Microbiol 2005;55:11–26. [PubMed: 15653847] (c) Clark BR, Engene N, Gerwick WH. J. Nat. Prod. 2008[In review]
16. Repetitive extraction with CH_2Cl_2/ CH_3OH (2:1) followed by normal phase vacuum liquid chromatography using organic mobile phase of increasing polarity generating nine fractions (A–I)
17. These fractions were initially active in a cell toxicity screen, but the activity did not repeat.
18. (a) FujIV K, Ikau Y, Oka H, Suzuki M, Harada K. Anal. Chem 1997;69:3346–3352. (b) FujIV K, Ikau Y, Oka H, Suzuki M, Harada K. Anal. Chem 1997;69:5146–5151. (c) Marfey P. Calsberg Res. Commun 1984;49:591–596.
19. Mamer OA. Meth. Enzymol 2000;324:3–10. [PubMed: 10989412]
20. Linington RG, Gonzalez J, Ureña LD, Romero LI, Ortega-Barría E, Gerwick WH. J. Nat. Prod 2007;70:397–401. [PubMed: 17328572]
21. (a) Geitler L. Akademische Verlagsgesellschaft 1932:942–943. (b) Komárek J, Anagnostidis K. Süsswasserflora von Mitteleuropa 2005;19/2:576–579.
22. Castenholz RW, Rippka R, Herdman M. Bergey's Manual of Systematic Bacteriology 2001;1:492–553.
23. Abed RM, Palinska KA, Camoin G, Gulobic S. FEMS Microbiol. Lett 2006;260:171–177. [PubMed: 16842341]
24. Sudek S, Haygood MG, Youssef DTA, Schmidt EW. Appl Environ Microbiol 2006;72:4382–4387. [PubMed: 16751554]
25. Van Wagoner R, Drummond AK, Wright JLC. Adv. Appl. Microbio 2007;61:89–217.
26. Katırcıoğlu H, Akın BS, Tahir A. African J. Biotech 2004;3:667–674.
27. Wilkinson CR, Sammarco PW. Mar. Ecol. Prog. Ser 1983;13:15–19.
28. (a) Mynderse JS, Moore RE, Kashiwagi M, Norton TR. Science 1977;196:538–540. [PubMed: 403608] (b) Mynderse JS, Moore RE. J. Org. Chem 1978;43:2301–2303.
29. Hooper GJ, Orjala J, Schatzman RC, Gerwick WH. J. Nat. Prod 1998;61:529–533. [PubMed: 9584405]
30. Edwards DJ, Marquez BL, Nogle JN, McPhail K, Goeger DE, Roberts MA, Gerwick WH. Chem. Biol 2004;11:817–833. [PubMed: 15217615]
31. Leusch H, Yoshida WY, Moore RE, Paul VJ. J. Nat. Prod 2000;63:1106–1112. [PubMed: 10978206]

NIH-PA Author Manuscript

NIH-PA Author Manuscript

NIH-PA Author Manuscript

32. (a) Gerwick WH, Roberts MA, Proteau PJ, Chen J-L. J. Appl. Phycol 1994;6:143–149. (b) Nubel U, Garcia-Pichel F, Muyzer G. Appl. Environ. Microbiol 1997;63:3327–3332. [PubMed: 9251225]

33. Buckner FS, Verlinde CL, LaFlamme AC, Van Boris WC. Antimicrob. Agents. Chemother 1996;40:2592–2597. [PubMed: 8913471]

34. Gutierrez M, Capson TL, Guzman HM, Gonzalez J, Ortega-Barria E, Quinoa E, Riguera R. J. Nat. Prod 2006;69:1379–1383. [PubMed: 17067146]

35. Calderon A, Romero L, Oretga-Barria E, Brun R, Correa M, Gupta MP. Panama Pharm. Biol 2006;44:1–16.

36. Kumar S, Tamura K, Nei M. Brief. Bioinform 2004;5:150–163. [PubMed: 15260895]

NIH-PA Author Manuscript

NIH-PA Author Manuscript

NIH-PA Author Manuscript

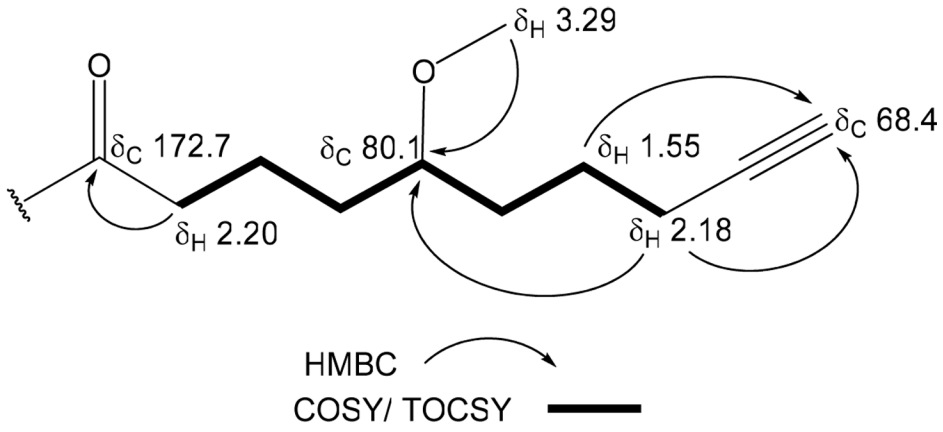

Figure 1.
The structure of the 5-methoxydec-9-ynoic acid moiety found in viridamides A (**1**) and B (**2**).

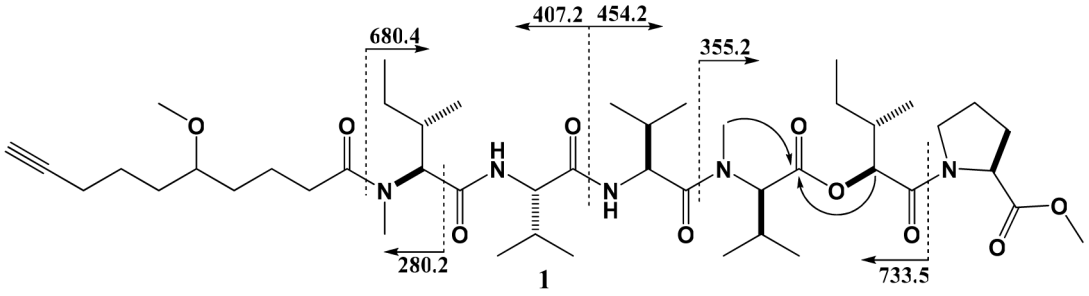

Figure 2.
Important fragmentations observed from FAB-MS and key HMBC connectivities used to sequence the series of residues in viridamide A (**1**).

NIH-PA Author Manuscript
NIH-PA Author Manuscript
NIH-PA Author Manuscript

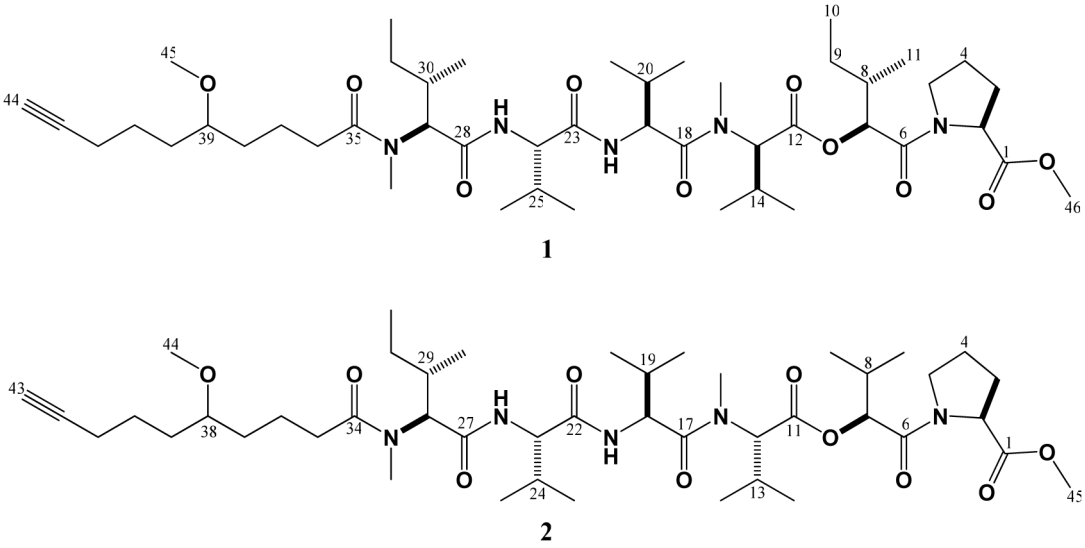

1

2

Figure 3.
The molecular structures of viridamides A (**1**) and B (**2**).

NIH-PA Author Manuscript NIH-PA Author Manuscript NIH-PA Author Manuscript

NIH-PA Author Manuscript
NIH-PA Author Manuscript
NIH-PA Author Manuscript

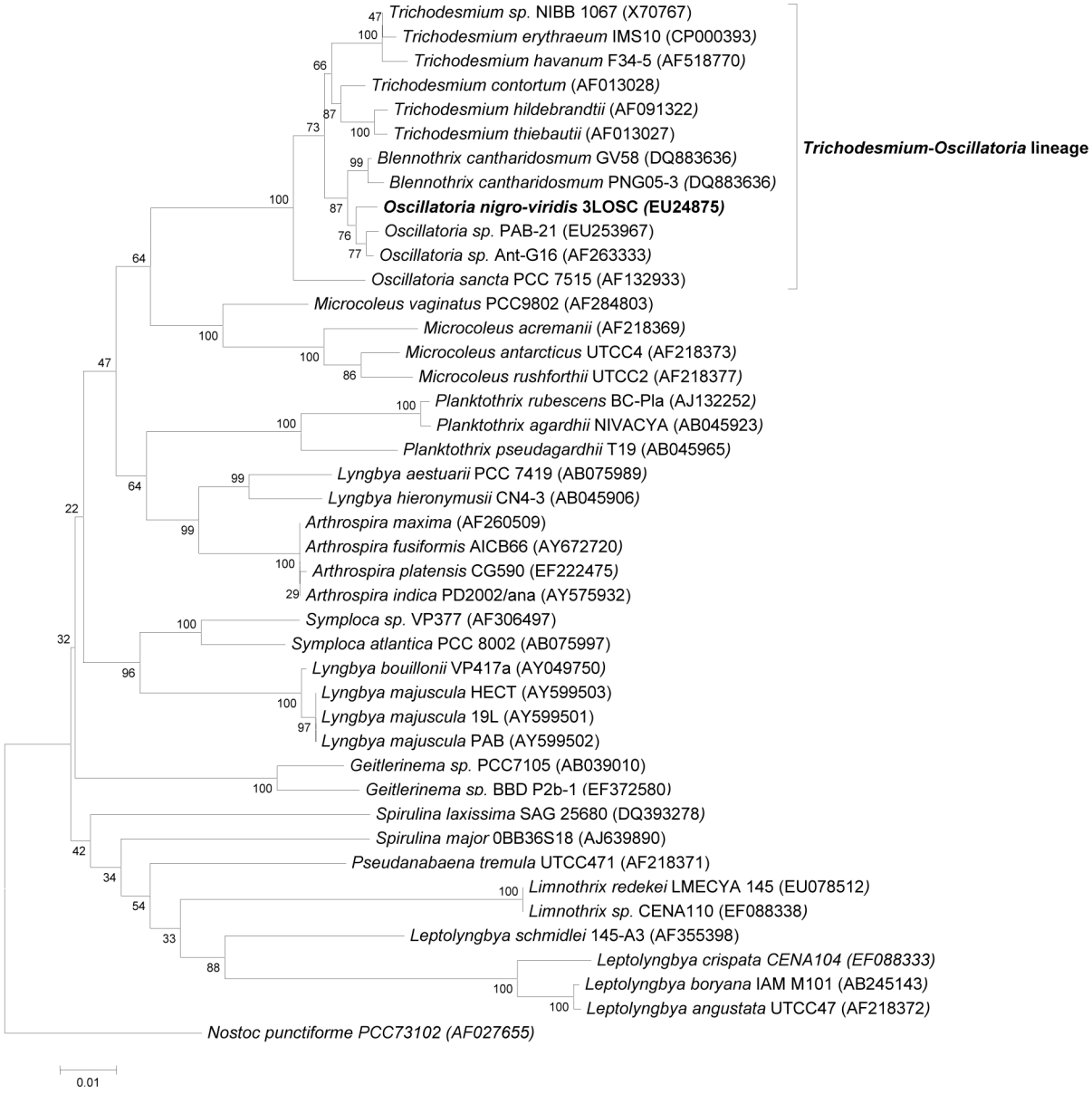

Figure 4.
The phylogenetic relationships of marine cyanobacteria of the order *Oscillatoriales* from 16S rDNA nucleotide sequences (ML).

NIH-PA Author Manuscript NIH-PA Author Manuscript NIH-PA Author Manuscript

Table 1

1D and 2D NMR data for viridamide A (**1**) in $CDCl_3$ (^1H NMR at 500 MHz; ^{13}C NMR at 75 MHz).

Residue	#	δ_C	δ_H(mult.)	gHMBC	gCOSY/TOCSY
Mdyna	44	68.4 (CH)			
	43	84.3 (C)			
	42	18.5 (CH_2)	2.18 (dd: 6.1, 6.3)	44,41,39	41
	41	24.1 (CH_2)	1.55 (m)	44	40,42
	40	32.3 (CH_2)	1.56 (m)		39,41
	39	80.1 (CH)	3.15 (m)		38,40
	38	32.8 (CH_2)	1.48 (m)	36	37,39
	37	21.5 (CH_2)	1.67 (m)		36,38
	36	36.6 (CH_2)	2.20 (m)	37,35	37
	35	172.7 (C)			
	45	56.4 (CH_3)	3.29 (s)	39	
***N*-Melle**	34	31.7 (CH_3)	3.07 (s)	35,29	
	29	60.7 (CH)	5.00 (d; 10.2)	28	30
	30	33.4 (CH)	1.96 (m)		29
	33	15.6 (CH_3)	0.96 (d; 6.8)	29	
	31	24.8 (CH_2)	1.0/1.34 (m)		
	32	10.77 (CH_3)	0.85 (dd; 6.5, 6.8)		
	28	172.9 (C)			
Val 1	NH		6.21	28	
	24	53.6 (CH)	4.81 (d; 6.3)	28	25
	25	31.2 (CH)	1.99 (td; 6.3, 6.5)		24
	26	17.4 (CH_3)	0.89 (d; 6.3)		
	27	19.6 (CH_3)	0.96 (d; 6.3)		
	23	169.5(C)			
Val 2	NH		6.45	23	

NIH-PA Author Manuscript
NIH-PA Author Manuscript
NIH-PA Author Manuscript

Residue	#	δ_C	δ_H(mult.)	gHMBC	gCOSY/TOCSY
	19	55.5 (CH)	4.58 (d; 6.8)	23	20
	20	30.8 (CH)	1.99 (td; 6.3, 6.8)		19
	21	19.7 (CH_3)	0.95 (d; 6.3)		
	22	17.7 (CH_3)	0.87 (d; 6.3)		
	18	170.3 (C)			
***N*-MeVal**	17	30.3 (CH_3)	3.01 (s)	18,13	
	13	62.1 (CH)	4.72 (d; 10.7)	12	14
	14	25.9 (CH)	2.27 (td; 6.5, 10.7)		13
	16	18.1 (CH_3)	0.78 (d; 6.5)		
	15	14.8 (CH_3)	0.88 (d; 6.5)		
	12	170.5 (C)			
Hmpa	7	74.9 (CH)	4.98 (d; 7.0)	9	8
	8	35.7 (CH)	2.01 (m)	7	7
	11	19.5 (CH_3)	0.95 (d; 6.3)		
	9	24.4 (CH_2)	1.19/1.61 (td; 6.3, 7.0)		
	10	10.8 (CH_3)	0.87 (t; 7.0)		
	6	170.0 (C)			
MePro	5	47.1 (CH_2)	3.52/3.92 (m)		
	4	24.5 (CH_2)	1.98/1.33 (m)		
	3	29.2 (CH_2)	1.97/2.14 (m)	2	
	2	58.6 (CH)	4.37 dd; 8.5, 3.4)	1	
	1	172.1 (C)			
	46	51.9 (CH_3)	3.64 (s)	1	

NIH-PA Author Manuscript NIH-PA Author Manuscript NIH-PA Author Manuscript

Table 2

1D and 2D NMR data for viridamide B (**2**) in $CDCl_3$ (^1H NMR at 500 MHz; ^{13}C NMR at 75 MHz).

Residue	#	δ_C	δ_H (mult.)	gHMBC	gCOSY/TOCSY
Mdyna	43	68.4 (CH)			
	42	84.3 (C)			
	41	18.5 (CH_2)	2.20 (dd; 6.0, 6.2)	43,40,38	40
	40	24.1 (CH_2)	1.56 (m)	43	39,41
	39	32.2(CH_2)	1.58 (m)		38,40
	38	79.3 (CH)	3.17 (m)		37,39
	37	32.8 (CH_2)	1.48 (m)	35	36.38
	36	21.5 (CH_2)	1.67 (m)		35,37
	35	36.8 (CH_2)	2.22 (m)	36,34	36
	34	172.8 (C)			
	44	55.8 (CH_3)	3.31 (s)	38	
***N*-MeIle**	33	31.5 (CH_3)	3.1 (s)	34,28	
	28	60.4 (CH)	5.03 (d; 10.1)	27	29
	29	33.5 (CH)	2.03 (m)		28
	32	15.6 (CH_3)	0.98 (d; 6.8)	28	
	30	24.8 (CH_2)	1.0/1.34 (m)		
	31	10.31 (CH_3)	0.85 (dd; 6.6, 6.7)		
	27	172.85 (C)			
Val 2	NH		6.19 (d; 9.3)	27	
	23	53.4 (CH)	4.86 (d; 6.4)	27	24
	24	29.3 (CH)	2.2 (td; 6.4, 6.6)		23
	25	17.4 (CH_3)	0.88 (d; 6.4)		
	26	19.6 (CH_3)	0.96 (d; 6.4)		
	22	169.6 (C)			
Val 1	NH		6.33 (d; 9.1)	22	

NIH-PA Author Manuscript
NIH-PA Author Manuscript
NIH-PA Author Manuscript

Residue	#	δ_C	δ_H (mult.)	gHMBC	gCOSY/TOCSY
	18	55.4 (CH)	4.59 (d; 6.7)	22	19
	19	30.8 (CH)	1.97 (td; 6.2, 6.7)		18
	20	19.6 (CH_3)	0.96 (d; 6.2)		
	21	19.6 (CH_3)	0.95 (d; 6.2)		
	17	172.1 (C)			
***N*-MeVal**	16	29.5 (CH_3)	2.99 (s)	17.12	
	12	61.4 (CH)	4.76 (d; 11.0)	11	13
	13	25.6 (CH)	2.27 (td; 6.4, 6.5)		11
	15	17.9 (CH_3)	0.81 (d; 6.4)		
	14	17.4 (CH_3)	0.88 (d; 6.4)		
	11	170.4 (C)			
Ahva	7	75.4 (CH)	4.96 (d; 6.8)	8	6
	8	33.4 (CH)	2.02 (m)	6	7
	10	19.6 (CH_3)	0.95 (d; 6.8)		
	9	18.1 (CH_3)	0.81 (d’ 6.1)		
	6	170.0 (c)			
MePro	5	46.8 (CH_2)	3.55/3.94 (m)		
	4	24.5 (CH_2)	1.99/2.05 (m)		
	3	28.9 (CH_2)	1.96/2.15 (m)	2	
	2	58.4 (CH)	4.38 (dd; 8.5, 2.5)	1	
	1	172.6 (C)			
	45	51.8 (CH_3)	3.66 (s)	1	

NIH-PA Author Manuscript NIH-PA Author Manuscript NIH-PA Author Manuscript

Table 3

Activity of viridamide A (**1**) against a series of pathogens (IC_{50}) and cancer cell lines (mm zones).

Compound	*T.cruzi*	*L.mexicana*	*P.falciparum*	HCT-116*	H-125*
	IC_{50} (μM)	IC_{50} (μM)	IC_{50} (μM)	aone (mm)	zone (mm)
1	1.1 ± 0.1	1.5 ± 0.15	1.5 ± 0.6	250	200
Nifurtimox	10 ± 0.5	-	-	-	-
Amphothericin B	-	0.1 ± 0.01	-	-	-
Chloroquine	-	-	0.1 ± 0.014	-	-

* indicates disk diffusion zone of inhibition